Journal of Molecular Graphics and Modelling 52 (2014) 103–113

Contents lists available at ScienceDirect

Journal of Molecular Graphics and Modelling

journal homepage: www.elsevier.com/locate/JMGM

Topical Perspectives

Allosteric pocket of the dengue virus (serotype 2) NS2B/NS3 protease: *In silico* ligand screening and molecular dynamics studies of inhibition

Azat Mukhametov[a,*], E. Irene Newhouse[b], Nurohaida Ab Aziz[a], Jennifer A. Saito[a], Maqsudul Alam[a,b,c,**]

[a] Centre for Chemical Biology, Universiti Sains Malaysia, 11800 Penang, Malaysia
[b] Advanced Studies in Genomics, Proteomics and Bioinformatics, University of Hawaii, 2565 McCarthy Mall, Honolulu, HI 96822, United States
[c] Department of Microbiology, University of Hawaii, 2538 McCarthy Mall, Honolulu, HI 96822, United States

ARTICLE INFO

Article history:
Accepted 20 June 2014
Available online 30 June 2014

Keywords:
Dengue
DENV2
NS2B/NS3 protease
Allosteric inhibitors

ABSTRACT

The allosteric pocket of the Dengue virus (DENV2) NS2B/NS3 protease, which is proximal to its catalytic triad, represents a promising drug target (Othman et al., 2008). We have explored this binding site through large-scale virtual screening and molecular dynamics simulations followed by calculations of binding free energy. We propose two mechanisms for enzyme inhibition. A ligand may either destabilize electronic density or create steric effects relating to the catalytic triad residues NS3-HIS51, NS3-ASP75, and NS3-SER135. A ligand may also disrupt movement of the C-terminal of NS2B required for inter-conversion between the "open" and "closed" conformations. We found that chalcone and adenosine derivatives had the top potential for drug discovery hits, acting through both inhibitory mechanisms. Studying the molecular mechanisms of these compounds might be helpful in further investigations of the allosteric pocket and its potential for drug discovery.

© 2014 Elsevier Inc. All rights reserved.

1. Introduction

Dengue virus (genus *Flavivirus)* is a human pathogen transmitted by the mosquitoes *Aedes aegypti* and *A. albopictus*. It poses a public health threat to 2.5 billion people worldwide, leading to 50–100 million human infections annually [1,2]. Approximately 500,000 dengue fever (DF) cases progress to dengue hemorrhagic fever (DHF) and dengue shock syndrome (DSS), resulting in ~25,000 deaths, mainly in children.

Dengue virus type 2 (DENV2) is the most prevalent of the four dengue serotypes [2]. The 10,723 nt genome of DENV2 encodes 3391 amino acid residues of a single polyprotein precursor C-prM-E-NS1-NS2A-NS2B-NS3-NS4A-NS4B-NS5 [3] (Fig. 1A).

DENV2 NS2B/NS3 is a serine protease of the trypsin superfamily with a catalytic triad (NS3-HIS51, NS3-ASP75 and NS3-SER135) [4]. DENV2 NS2B/NS3 protease is a complex of two separate proteins – the NS2B protein and the protease domain of the NS3 protein [5]. Forty amino acid residues of the hydrophilic segment of NS2B are vital for structural stability and enzymatic activity [5,6]. The protease adopts two critical conformational states – a "closed" conformation in which the C-terminal of NS2B is bound to the allosteric pocket proximal to the catalytic triad, and an "open" conformation with the NS2B chain coiled with its C-terminal away from the allosteric pocket (Fig. 1B). It has been proposed that the "open" structural conformation is favored in the DENV2 NS2B/NS3 protease [7,8]. Based on the published data, it has been postulated that there are several stages in native enzyme activity: "open" conformation > substrate binding > reaction > motion of the C-terminal of NS2B into the "closed" conformation > release of reaction products > return to the "open" conformation [5–10]. Our analysis of the homology model of the "closed" conformation of the protease [11] reveals an essential role for NS3-ASN152 in keeping the C-terminal of the NS2B chain fixed in the allosteric pocket of the NS3 protease domain.

NS2B-GLY_4-SER-GLY_4-NS3pro, which is commonly used in experimental studies, shows decreased enzymatic activity compared to the native DENV2 NS2B/NS3 protease [12]. This is likely due to it being fixed in the "open" conformation.

Few allosteric inhibitors of DENV2 NS2B/NS3 protease have been experimentally identified, and their binding modes were elucidated through *in silico* docking [13,14]. We conclude that NS3-LYS74, NS3-LEU149, and NS3-ASN152 are essential for interactions with inhibitors.

* Corresponding author. Tel.: +60 4 653 55 00; fax: +60 4 653 55 14.
** Corresponding author. Tel.: +1 808 956 81 21; fax: +1 808 958 09 25.
E-mail addresses: azatccb@gmail.com (A. Mukhametov), alam@hawaii.edu (M. Alam).

http://dx.doi.org/10.1016/j.jmgm.2014.06.008
1093-3263/© 2014 Elsevier Inc. All rights reserved.

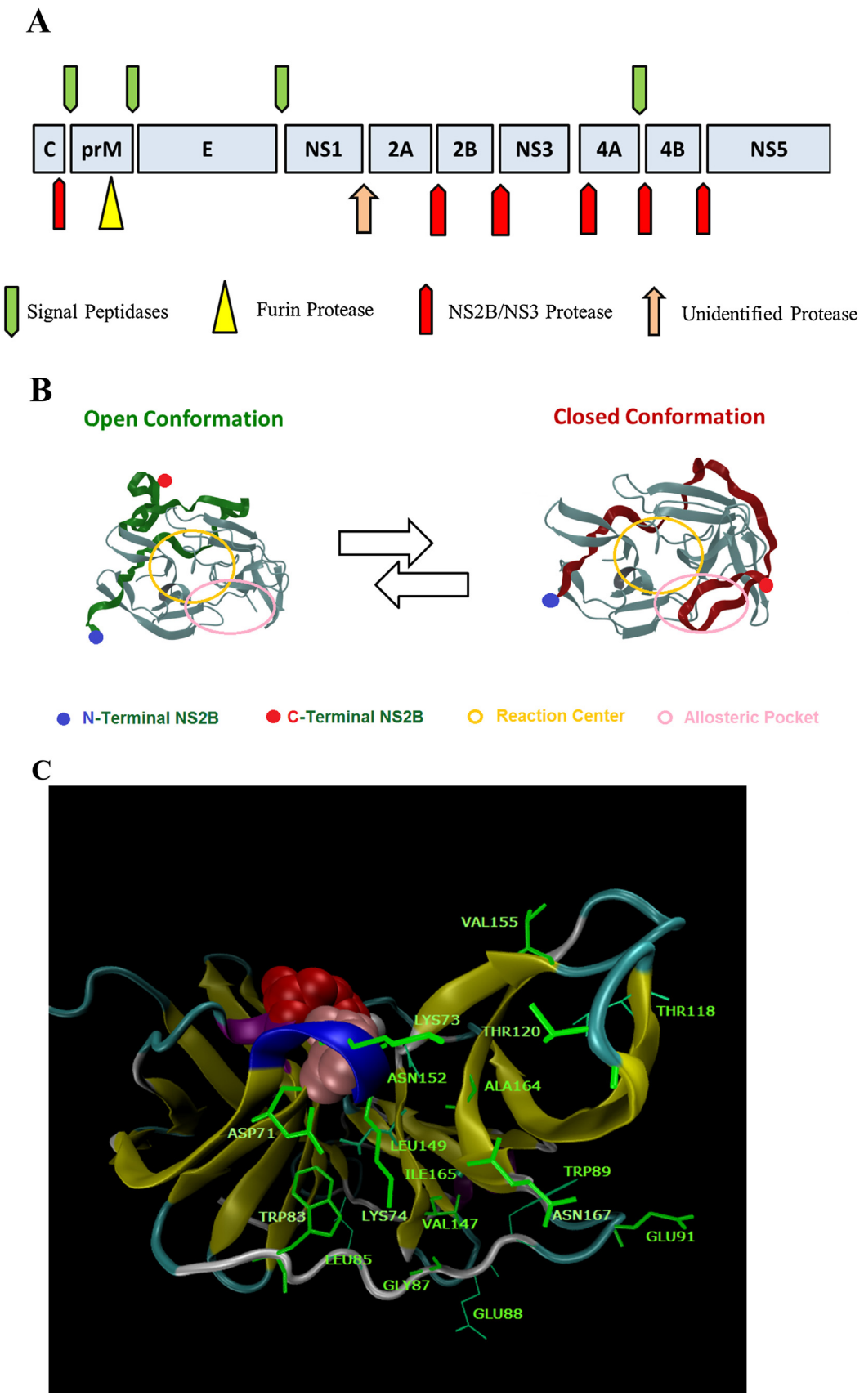

Fig. 1. Function and structure of DENV2 NS2B/NS3 protease. (A) Proteins comprising DENV polyprotein sequence, and enzymes in charge of its cleavage; (B) feasible role of "open"–"closed" conformational move in protease function in native condition. (C) Molecular structure of DENV2 NS2B/NS3 protease: reaction center residues are shown in VDW representation – NS3-ASP75 (pink), NS3-HIS51 (red), and NS3-SER135 (gray, behind); residues of the allosteric pocket in NS3 domain are shown with green lines – NS3-ASP71, NS3-LYS73, NS3-LYS74, NS3-TRP83, NS3-LEU85, NS3-GLY87, NS3-GLU88, NS3-TRP89, NS3-GLU91, NS3-THR118, NS3-THR120, NS3-VAL147, NS3-LEU149, NS3-ASN152, NS3-VAL155, NS3-ALA164, NS3-ILE165, and NS3-ASN167. (For interpretation of the references to color in this figure legend, the reader is referred to the web version of the article.)

In this work, we have identified ligands that bind to the allosteric pocket of the DENV2 NS2B/NS3 protease, and present potential molecular mechanisms involved in protease inhibition.

2. Methods

2.1. Preparation of the protein and ligand structural data

The structure of DENV2 NS2B/NS3 protease was retrieved from the PDB database (http://www.pdb.org, ID: 2FOM) [15]. Missing residues were filled in with the Prime Suite of Schrödinger [16]. The first 3 residues of the N-terminal of NS2B were truncated to decrease protein volume fluctuations, and the final structure was prepared using the Schrödinger Protein Preparation Wizard [16]. The structure of the DENV2 NS2B/NS3 protease was assessed by the Schrödinger SiteMap [16] utility using default settings. The highest-scoring site coincided with the previously identified allosteric pocket [14].

Ligand databases were downloaded from the ZINC website (http://zinc.docking.org) [17] and commercial vendor websites, and were prepared using the Schrödinger LigPrep application [16].

2.2. Virtual screening of small molecule databases

The structure of DENV2 NS2B/NS3 protease (http://www.pdb.org, ID: 2FOM) prepared according to Section 2.1 was used for virtual screening.

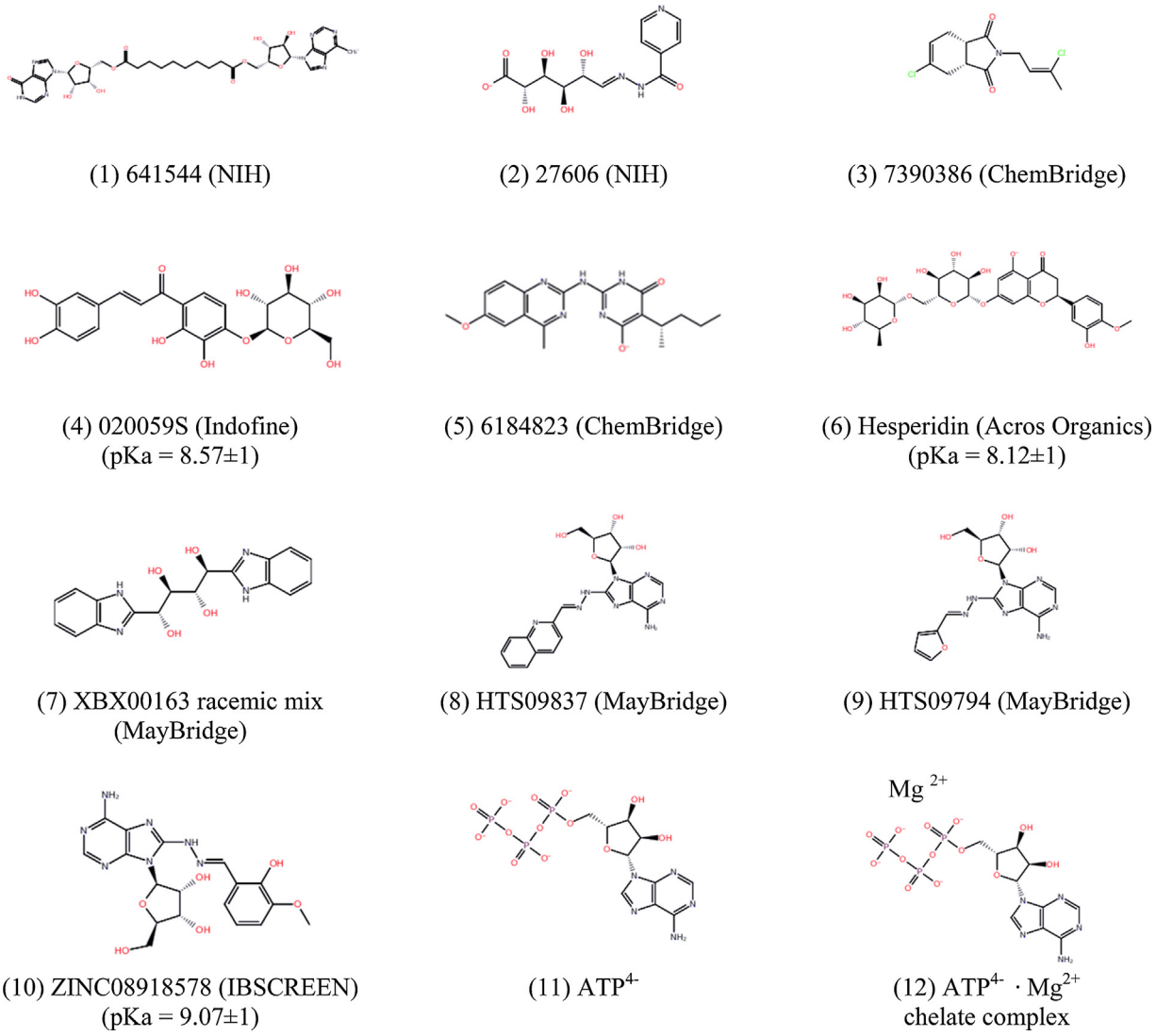

Fig. 2. Allosteric inhibitors of DENV2 NS2B/NS3 protease. Structural formulas[a,b] of compounds (1)–(12) and their catalog numbers in vendor databases are shown. ([a] Depicted are tautomerization/ionization states dominant at pH 8.5 (predicted by Schrödinger Software package). [b] Respective chemical names of the structures shown are: **(1)** 1-[(2R,4R,5R)-5-(6-amino-7-hydroxy-3H-imidazo[4,5-b]pyridin-3-yl)-3,4-dihydroxytetrahydro-2-furanylmethyl] 10-[(2R,3S,4S,5R)-3,4-dihydroxy-5-(6-oxo-6,9-dihydro-1H-9-purinyl)tetrahydro-2-furanylmethyl] sebacate; **(2)** (2S,3S,4R,5R)-2,3,4,5-tetrahydroxy-6-(4-pyridylcarbonylhydrazono)hexanoic acid; **(3)** (3aR,7aS)-5-chloro-2-[(Z)-3-chloro-2-butenyl]-2,3,3a,4,7,7a-hexahydro-1H-1,3-isoindoledione; **(4)** (E)-3-(3,4-dihydroxyphenyl)-1–2,3-dihydroxy-4-[(1R,2S,3S,4R,5R)-2,3,4-trihydroxy-5-hydroxymethylcyclohexyloxy]phenyl-2-propen-1-one; **(5)** 2-(6-ethyl-4-methyl-2-quinazolinylamino)-4-hydroxy-5-[(1S)-1-methylbutyl]-1,6-dihydro-6-pyrimidinone; **(6)** (2S)-5-hydroxy-2-(3-hydroxy-4-methoxyphenyl)-7-(1R,2S,3S,4R,5R)-2,3,4-trihydroxy-5-[(1R,2S,3R,4S,5R)-2,3,4-trihydroxy-5-methylcyclohexyloxymethyl]cyclohexyloxy-3,4-dihydro-2H-4-chromenone; **(7)** (1R,2R,3S,4S)-1,4-di(1H-benzo[d]imidazol-2-yl)butane-1,2,3,4-tetraol; **(8)** 2-quinolinecarbaldehyde N-{6-amino-9-[(2R,3R,4S,5R)-3,4-dihydroxy-5-(hydroxymethyl)tetrahydro-2-furanyl]-9H-purin-8-yl}hydrazine; **(9)** 2-furaldehyde N-{6-amino-9-[(2R,3R,4S,5R)-3,4-dihydroxy-5-(hydroxymethyl)tetrahydro-2-furanyl]-9H-purin-8-yl}hydrazine; **(10)** 2-hydroxy-3-methoxybenzaldehyde N-{6-amino-9-[(2R,3R,4S,5R)-3,4-dihydroxy-5-(hydroxymethyl)tetrahydro-2-furanyl]-9H-purin-8-yl}hydrazine; **(11)** [(2R,3S,4R,5R)-5-(6-aminopurin-9-yl)-3,4-dihydroxyoxolan-2-yl]methyl-(hydroxyphosphonooxyphosphoryl)hydrogen phosphate; **(12)** [(2R,3S,4R,5R)-5-(6-aminopurin-9-yl)-3,4-dihydroxyoxolan-2-yl]methyl(hydroxyphosphonooxyphosphoryl) hydrogen phosphate magnesium salt).

Grid preparation and virtual screening were performed using Schrödinger Glide [16] and the Virtual Screening Workflow [16], respectively. Tautomeric forms were proposed by the Epik application of the Schrödinger LigPrep tool [16] during ligand preparation.

Compounds from the ZINC Database [17], comprising the Natural Compounds DB, the NCBI Plated DB, ChemBridge, TimTec, MayBridge, IBSCREEN, and others were screened virtually against the allosteric pocket of the DENV2 NS2B/NS3 protease. The target site included residues NS3-ASP71, NS3-LYS73, NS3-LYS74, NS3-TRP83, NS3-LEU85, NS3-GLY87, NS3-GLU88, NS3-TRP89, NS3-GLU91, NS3-THR118, NS3-THR120, NS3-VAL147, NS3-LEU149, NS3-ASN152, NS3-VAL155, NS3-ALA164, NS3-ILE165, and NS3-ASN167 (Fig. 1C).

Representative set of compounds was selected with the purpose to represent structural scaffolds appeared during virtual screening. Compounds with top Glide Score values were studied through the perspective binding ways and only scaffolds which could create maximum number of interactions with allosteric binding site were included. Structures with intuitively low chemical stability were not included into representative set. Compounds were additionally filtered using QikProp application of Schrodinger package [16] for solubility and metabolic stability.

Hydrogen bonds in protein–ligand complexes, generated through virtual screening, were identified with Maestro application of Schrodinger package [16] using the criteria: donor–acceptor distance between the heavy atoms of up to 3.5 Å and 60° for the angle cutoff.

Figures of the protein–ligand complexes were prepared using the VMD software [18].

2.3. Molecular dynamics simulations

Molecular dynamics simulations were performed for the structures of selected protein – ligand complexes which had been generated through virtual screening against the structure of DENV2 NS2B/NS3 protease (http://www.pdb.org, ID: 2FOM).

Protein and ligand structures were assessed using the PDB2PQR server [19] to predict the solution protonation states of the protein

Table 1
Hydrogen bonds interaction fingerprints for DENV2 NS2B/NS3 protease allosteric inhibitors. Colored map shows the hydrogen bond contacts between the protein and ligand structures in the protein–ligand complexes[a] resulting from docking.

CPD# / pose	GScore	NS3-ASP 71	NS3-LYS 73	NS3-LYS 74	NS3-TRP 83	NS3-LEU 85	NS3-GLY 87	NS3-GLU 88	NS3-TRP 89	NS3-GLU 91	NS3-THR 118	NS3-THR 120	NS3-VAL 147	NS3-LEU 149	NS3-ASN 152	NS3-VAL 155	NS3-ALA 164	NS3-ILE 165	NS3-ASN 167
(1)/a	-12.711																		
(1)/b	-11.845																		
(2)/a	-11.267		++																
(2)/b	-11.56																		
(3)/a	-7.958																		
(3)/b	-6.374																		
(4)/a	-13.602																		
(4)/b	-10.09																		
(5)	-7.721														+++				
(6)/a	-13.68																		
(6)/b	-13.618	++																	
(7)/a	-11.019		++												++				+++
(7)/b	-13.568																		++
(8)	-13.91													++					++
(9)	-13.03													++	+++				+++
(10)	-16.11			++										++	++				
(11)	-12.633														++				
(12)	-9.799																		

Residue is acceptor Residue is donor Residue is acceptor and donor

[a] When there is more than one hydrogen bond between the ligand molecule and the amino acid residue, their number is marked by the number of "+" signs.

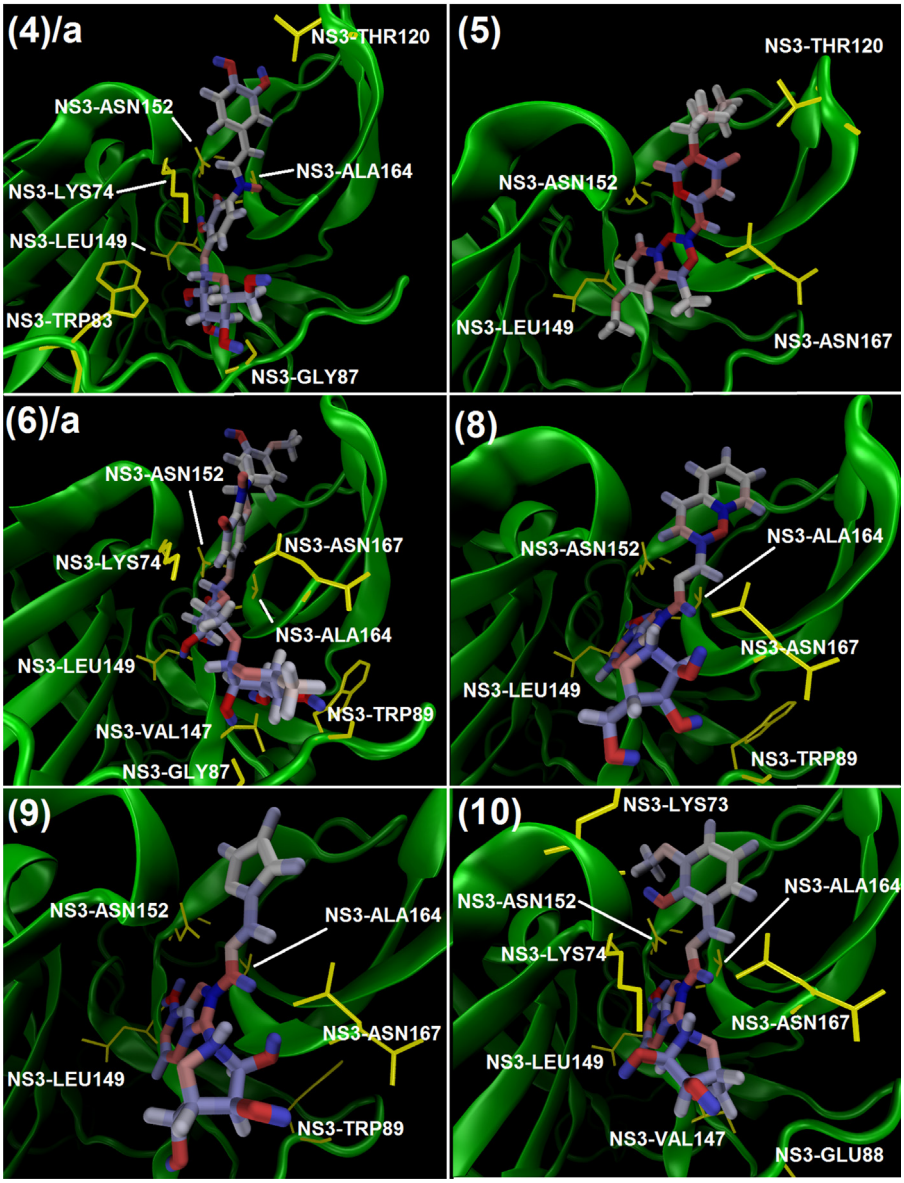

Fig. 3. Binding poses for the allosteric inhibitors of DENV2 NS2B/NS3 protease. Compounds (4)/a, (5), (6)/a, (8), (9), and (10) bound to the allosteric site are shown (colored in electronegativity representation), interacting amino acids are represented in yellow lines, protein backbone is green. (For interpretation of the references to color in this figure legend, the reader is referred to the web version of the article.)

bound to ligand. Ligand parameters for PDB2PQR were estimated with the SwissParam Server [20]. Molecular dynamics (MD) simulations were executed using NAMD [21]. The Amber Tools package [22] was used to prepare input data. Prior to preparing the DENV2 NS2B/NS3 protease structure by the XLEAP application of AMBER [22], hydrogens were deleted using Maestro (Schrödinger Package) [16]. Structures of protein and ligand–protein complexes were neutralized by adding Na^+ and Cl^- ions, and additional Na^+Cl^- ions were added to attain 0.15 M ionic strength. A 12 Å water box of explicit solvent model TIP3PBOX water was applied. The protein was prepared using the FF99SB force field. General Amber Force Field (GAFF) parameters were assigned to ligands, while partial charges were calculated using the AM1-BCC method as implemented in the Antechamber suite of the AMBER11.0 software package [22].

Energy minimization, heating, density equilibration and four stages of harmonically restrained MD preceded unrestrained production stages. The system was minimized in three stages using the conjugate gradient algorithm: with fixed protein and ligand; with fixed protein atoms; with fixed protein backbone. The protein backbone was restrained during the heating and density equilibration stages. Harmonic constraints were applied on backbone atoms with scaling 1.0, 0.75, 0.5, and 0.25 during the four stages of harmonically restrained MD. The system was heated from 0 to 300 K in 500,000 steps with temperature reassignment, and a Langevin thermostat with a collision frequency of 5.0 ps^{-1} was used for subsequent temperature maintenance. The density was equilibrated in 50,000 steps (50 ps) with Langevin piston pressure control (1.01325 bar, 300 K). All MD simulations were performed with a 1.0 fs time step and a cutoff of 12.0 Å for non-bonded interactions.

Production MD was run for 5 and 10 ns for the complex and apo-protein structures, respectively.

Trajectory analysis was done with the PTRAJ application of Amber Tools [22]. RMSD plots were drawn using the XMGRACE software [23].

2.4. MM PB/GBSA calculations

Assessments of the free energy of protein–ligand binding (dG) were performed using MM PB/GBSA approaches, as implemented in the MMPBSA program of Amber Tools [22]. Enthalpy terms were calculated by both PBSA and GBSA methods on 250 snapshots taken at regular intervals from 3.0 to 5.0 ns trajectory. Six equally spaced snapshots were used from the same trajectory segment to calculate entropy terms by normal mode analysis.

2.5. Calculation of hydrogen bonds occupancies

Hydrogen bonds occupancies during the unrestrained 5 ns molecular dynamics simulations for the complexes of DENV2 NS2B/NS3 protease and the allosteric inhibitors were calculated using VMD extension for H-bond analysis [18]. Calculations were performed for each protein–ligand complex, using the parameters for H-bond detection: donor–acceptor distance between heavy atoms of 3.5 A and 60 deg. for the angle cutoff.

2.6. Preliminary in vitro assessment of inhibitory activity

A recombinant DENV2 NS2B/NS3 protease was prepared as described previously [24]. Protease activity experiments were performed *in vitro* using purified recombinant DENV2 NS2B/NS3 protease and 7-amino-4-methylcoumarin (AMC) fluorophore-linked peptide substrate BOC-GRR-AMC following a published procedure [25]. Stock solution (10 mM) of BOC-GRR-AMC (Peptide Institute, Japan) was prepared by dissolving the peptide in DMSO. This was then diluted in water to a 1 mM working stock. Inhibitory activity studies were performed by incubating 100 μM of each compound with 0.05 mg/ml recombinant DENV NS2B-NS3pro in assay buffer (200 mM Tris [pH 8.5], 20% glycerol) for 15 min at 25 °C. Then, 100 μM BOC-GRR-AMC was added and the incubation continued for an additional 30 min. Release of free AMC was monitored at excitation and emission wavelengths of 380 and 450 nm, respectively. Positive (100 μM aprotinin) and negative/untreated controls were run along with the assay.

3. Results and discussion

The allosteric pocket [14], which is proximal to the catalytic triad (Fig. 1C), was explored by means of automated docking, molecular dynamics simulations and free energy calculations. Two possible molecular mechanisms underlying allosteric inhibition of the DENV2 NS2B/NS3 protease were studied: (a) allosteric binding creates hindrances for substrate interaction with the catalytic triad, or through modulating activity by electron withdrawal or other mechanisms [14]; and (b) the inhibitor interferes with motion of the C-terminal of NS2B into the allosteric pocket during formation of the "closed" protein conformation (suggested as a stage necessary for the release of protease reaction products [10]).

The ability of ligands to inhibit the DENV2 NS2B/NS3 protease by the first mechanism was assessed *in silico* through docking ligands into the 2FOM.pdb structure followed by binding modes analysis and calculation of the free energy of binding. The second mechanism was studied by using the published homology model of the "closed" conformation of the DENV2 NS2B/NS3 protease [11] for superposition studies.

3.1. Structures of allosteric inhibitors

Site mapping of the DENV2 NS2B/NS3 protease structure revealed a SiteScore of 0.975 for the allosteric pocket area, which was much higher than that calculated for the catalytic triad (Fig. 1C).

Among the hits identified during virtual screening, twelve compounds (Fig. 2) were selected for further investigation. The representative set included two chalcones (compounds 4, 6) and three adenosine (compounds 8–10) derivatives. Other chalcones have previously been identified as allosteric inhibitors [13,14]. These observations indicate that the allosteric pocket might preferably bind these scaffolds. The synthetic adenosine derivatives (compounds 8–10) may interfere with natural nucleosides. Thus we docked a nucleoside library, and adenosine triphosphate was found to be the top hit (compounds 11, 12).

3.2. Hydrogen bonds interactions

Analysis of the protein–ligand complex structures from virtual screening revealed that NS3-ASN152, NS3-ASN169, NS3-ALA164, and NS3-LEU149 were the main allosteric pocket residues interacting with inhibitors (Table 1). It is interesting, that while compounds (1), (2), and (4) could bind NS2B/NS3 protease in multiple ways, the others had primarily one or two binding modes.

Based on the Glide Score values (Table 1), the binding ability of the compounds were ordered as: ZINC08918578 > HTS09837 > Hesperedin > 020059S > XBX00163 > HTS09794 > 641544 > ATP^{4-} > 27606 > $ATP^{4-}{\cdot}Mg^{2+}$ > 7390386 > 6184823 (compounds 10, 8, 6, 4, 7, 9, 1, 11, 2, 12, 3, 5, respectively).

3.3. Binding poses for ligands

Due to molecular flexibility, the sugar-bound flavone (compound 4) could assume different positions inside the allosteric pocket. Only those close to NS3-ASN152 of the NS3 chain were considered to be active in allosteric inhibition (Fig. 3). A "horizontal" position, in which the ligand stretched between NS3-ALA164 and NS3-LEU149, with higher GScore value (−10.09 *vs.* −13.602) was not considered as effectively inhibitory (Supplementary Information: Fig. S1, pose (4)/b).

At pH 8.5, compound (5) was predicted to dissociate into the tautomeric form shown in Fig. 2. It might assume two poses inside the binding pocket, both creating strong hydrogen bonding to NS3-ASN152. The pose with the hydrophobic Met-O-group rotated into water is probably the more favorable binding mode (Fig. 3).

Docking of hesperidin (compound 6), a well-known molecule of natural origin with various applications in medicine, revealed that it could bind to the allosteric pocket of the DENV2 NS2B/NS3 protease in two ways: with the substituent phenyl group rotated inside, into the binding pocket (Fig. 3, pose (6)/a), or outside, into the water area (Supplementary Information: Fig. S1, pose (6)/b). We expect that binding mode (6)/a, with a slightly more negative GScore value, may be dominant (−13.680 *vs.* −13.618).

Adenosylhydrazine derivatives (8)–(10) had only one binding mode (Fig. 3). The adenine ring was positioned inside the bottom of the allosteric pocket, creating hydrogen bonds with NS3-LEU149 and NS3-ASN152, and the ribose group was rotated toward water. The substituents to the adenosylhydrazine scaffold were found to be located at the top part of the allosteric pocket, close to the reaction center and two large loops (Fig. 3).

According to the docking results, 2-hydroxy-3-methoxybenzaldehyde N-adenosylhydrazine (compound 10) fits best into the allosteric binding pocket due to the hydroxyl group in the phenyl ring, which creates a hydrogen bond to NS3-LYS73 that is proposed to be essential for inhibition [14] (Fig. 3), and the Met-O-group which orients toward the solvent.

Although the binding strength of the 2-quinolinecarbaldehyde derivative (compound 8) was lower than that of the 2-hydroxy-3-methoxybenzaldehyde derivative (compound 10), the bulky

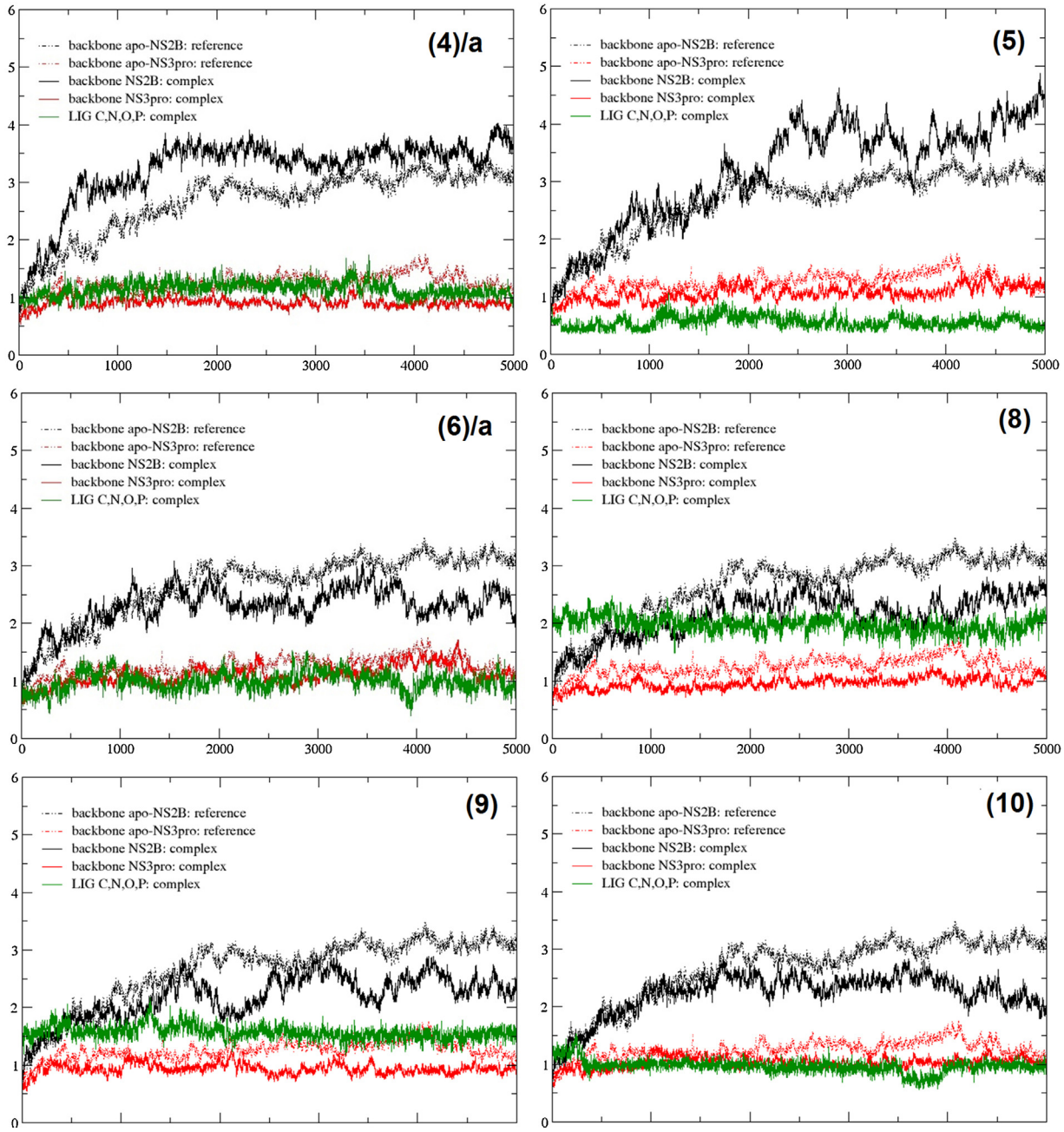

Fig. 4. RMSD plots during 5 ns unrestrained molecular dynamics simulations for the complexes of the ligands with the allosteric pocket of DENV2 NS2B/NS3 protease. Data for the compounds (4)/a, (5), (6)/a, (8), (9), and (10) bound to the allosteric site are shown.

pyridinyl substituent might perturb protease activity through steric and, possibly, electron-withdrawal mechanisms (Fig. 3).

3.4. Protein and ligand structure stability

MD simulation performed with the apo-NS2B/NS3 protease for 10 ns demonstrated that the NS3 chain coordinates were highly stable, while the NS2B chain equilibrated within the first 2 ns of the production stage (Supplementary Information: Fig. S2). Based on these results we concluded that the MD settings used for the apo-protein could be used to simulate the DENV2 NS2B/NS3 protease – ligand complexes with minor modifications.

MD simulations (5 ns) were performed for the DENV2 NS2B/NS3 protease – ligand complexes (Fig. 4; Supplementary Information: Fig. S3). All poses were found to be stable during the course of MD simulation. However NS2B moved more when the ligand was secondary amine 6184823 or tetraol XBX00163 (Fig. 4, compound 5; Supplementary Information: Fig. S3, compound (7)/b, respectively). The lowest RMSD was observed for the complexes with substituted adenosylhydrazines (compounds 8–10) (Fig. 4).

According to analysis of the RMSD plots (Fig. 4; Supplementary Information: Fig. S3), calculated from MD simulations of the protein–ligand complexes, the presence of any ligand in the protease allosteric pocket stabilized the NS3 protease domain. However, the influence on the NS2B chain depended on the ligand. Compounds (3)/b, (6), (8), (9), and (10) stabilized the crystal conformation of the NS2B chain, while compounds (2), (4)/a, (5), and (7)/b had a destabilizing effect. The remaining ligand poses ((1)/a/b, (3)/a, (4)/b, and (7)/a) did not show any evident influence on the NS2B chain conformation. All of the ligands studied were found

Table 2
Energetic characteristics of binding of different inhibitors (1)–(12) in various modes to the allosteric pocket of DENV2 NS2B/NS3 protease. Results from enthalpy, entropy, and Gibbs energy calculations using GBSA and PBSA methods are shown.[a]

CPD/pose	MM PB/GBSA AMBER Prediction				
	$dH_{250p.of\ 3\text{-}5\ k}{}^{GBSA}$	$TdS_{6\ p.of\ 3\text{-}5\ k}$	dG^{GBSA}	$dH_{250\ p.of\ 3\text{-}5\ k}{}^{PBSA}$	dG^{PBSA}
(1)/a	−38.93 ± 4.31	−28.38 ± 4.87	−10.55	−27.34 ± 5.34	1.04
(1)/b	−39.6 ± 4.3	−29.33 ± 6.65	−10.27	−30.33 ± 4.75	1.00
(2)/a	−21.57 ± 3.74	−20.28 ± 2.97	−1.29	−13.56 ± 5.0	6.72
(2)/b	−19.43 ± 4.64	−25.76 ± 8.81	6.31	−10.36 ± 4.48	15.4
(3)/a	−31.54 ± 2.38	−17.31 ± 5.16	−14.23	−26.90 ± 2.85	−9.59
(3)/b	−26.3 ± 3.9	−23.71 ± 2.20	−2.59	−20.33 ± 3.95	3.38
(4)/a	−29.90 ± 4.40	−20.72 ± 6.15	−9.18	−7.33 ± 8.27	13.39
(4)/b	−29.43 ± 3.58	−18.24 ± 5.90	−11.19	−18.30 ± 4.05	−0.06
(5)	−30.0 ± 4.7	−26.22 ± 3.4	−3.78	23.15 ± 8.26	49.37
(6)/a	−44.66 ± 5.8	−25.63 ± 3.3	−19.03	−29.66 ± 6.87	−4.02
(6)/b	−25.2 ± 4.14	−22.37 ± 8.19	−3.33	−10.94 ± 5.76	11.43
(7)/a, RRRR	−21.25 ± 3.24	−21.47 ± 2.02	0.22	−12.53 ± 5.56	8.94
(7)/b, RRRS	−18.53 ± 3.1	−21.37 ± 4.19	2.84	−10.19 ± 3.50	11.18
(8)	−33.56 ± 3.1	−26.21 ± 2.44	−7.35	−28.89 ± 5.11	−2.68
(9)	−35.11 ± 2.97	−20.18 ± 3.38	−14.93	−27.62 ± 4.52	−7.44
(10)	−51.03 ± 3.91	−26.01 ± 2.29	−24.02	−40.46 ± 4.71	−14.45
(11)	−3.29 ± 4.65	−25.02 ± 1.70	21.73	2.41 ± 8.75	27.43
(12)	−15.01 ± 6.05	−19.23 ± 5.16	4.22	−18.60 ± 7.76	0.63

[a] Data given in Kcal/M, standard deviation is shown as ± values.

to be quite stable over the course of MD simulation, except compound (1). It had a tendency for large fluctuations, possibly because of its very flexible and long chemical structure (Supplementary Information: Fig. S3).

3.5. Free energy of protein-ligand binding

The calculated dG_{bind} values for the protein–ligand complexes generally correlated with the GScore values for the chalcone/stilbene and adenosine scaffolds retrieved (Table 2). Thus, free energy calculations using the Generalized Born solvation model (GBSA) approach ordered the binding strength of ligands to the DENV2 NS2B/NS3 protease allosteric site as: ZINC08918578 > Hesperidin > HTS09794 > 7390386 > 020059S > 641544 > HTS09837 > 6184823 > 27606 > XBX00163 > $ATP^{4-}{\cdot}Mg^{2+}$ > ATP^{4-} (compounds 10, 6, 9, 3, 4, 1, 8, 5, 2, 7, 12, and 11, respectively). The Poisson-Boltzmann model (PBSA) ordered the compounds as ZINC08918578 > 7390386 > HTS09794 > Hesperidin > HTS09837 > 020059S > $ATP^{4-}{\cdot}Mg^{2+}$ > 641544 > 27606 > XBX00163 > ATP^{4-} > 6184823 (compounds 10, 3, 9, 6, 8, 4, 12, 1, 2, 7, 11, and 5, respectively; Table 2).

The positive dG_{bind} values, calculated for the adenosine triphosphate molecules, possibly indicate limitations in the free energy assessment methods, as experimental testing demonstrated 25 and 27% of inhibition for ATP^{4-} and $ATP^{4-}{\cdot}Mg^{2+}$, respectively (see below).

3.6. Hydrogen bond occupancy in MD simulation

The MD simulation trajectories of the protein–ligand complexes were also used to calculate the occupancies of hydrogen bonds between the protein and ligands (Fig. 5). The hydrogen bond networks around each ligand stabilized over the course of MD simulation, with the list of interacting residues remaining nearly the same. As in the initially docked binding poses, NS3-ASN152, NS3-LEU149, NS3-ASN167, and NS3-ALA164 continued to be the primary interacting residues. In the initial docking poses, residues could be ordered according to the number of hydrogen bonding events in which they participated as NS3-ASN152 (15 events) > NS3-ASN167 (11 events) > NS3-LEU149 (10 events) > NS3-ALA164 (8 events). In the MD simulations they were reordered as NS3-ASN167 (14 events) > NS3-ASN152 (13 events) > NS3-LEU149 (13 events) > NS3-ALA164 (8 events). It is interesting that while the occupancies of many hydrogen bonds were less than 100% (NS3-ASN152, NS3-ASN167), NS3-LEU149 and NS3-ALA164 retained or even increased hydrogen-bonding strength (Fig. 5).

3.7. Experimental data

In preliminary *in vitro* assessments (Fig. 6), the 2-hydroxy-3-methoxybenzaldehyde N-adenosinylhydrazine (compound 10) inhibited the DENV2 NS2B/NS3 protease the most (65.1%; Fig. 6), followed by the glucose-substituted stilbene 020059S (compound 4, 61.5%).

The activity of all the compounds could be arranged as ZINC08918578 > 020059S > HTS09837 > 6184823 > HTS09794 > 641544 > Hesperidin > $ATP^{4-}{\cdot}Mg^{2+}$ > 27606 > 7390386 > ATP^{4-} > XBX00163 (compounds 10 (65.1%), 4 (61.5%), 8 (59.2%), 5 (54.5%), 9 (46.9%), 1 (36.2%), 6 (31.4%), 12 (27.1%), 2 (25.8%), 3 (24.6%), 11 (24.7%), 7 (23.8%), respectively; Fig. 6)).

According to the experimental data, the nature of the substituent in N-adenosinylhydrazines plays an important role in the activity. The data shows that the influence of substituents on the percentage of inhibition may be ordered as follows: p-methoxy-o-hydroxyphenyl-R (compound 10; 65.1% protease inhibition) > pyridinyl-R (compound 8; 59.2% inhibition) > furanyl-R (compound 9; 46.9% inhibition). We conclude that the smallest and the least electro-negative furanyl substituent in compound (9) could not perturb enzymatic activity as much as the substituents in compounds (10) and (8).

Low activity of ATP in the experimental study (25 and 27% of protease inhibition for ATP^{4-} and $ATP^{4-}{\cdot}Mg^{2+}$, respectively; Fig. 6), compared to the synthetic adenosine derivatives (compounds 8, 9, and 10 with experimental inhibition values of 59.2, 46.9, and 65.1%, respectively; Fig. 6), suggests that native ATP-related biochemical processes may not seriously compete with synthetic adenosine derivatives for the allosteric site. In addition, synthetic adenosine derivatives may not be influenced in ATP-related biochemical processes, due to inherited differences in binding profile of these molecular structures.

3.8. Mechanism of allosteric inhibition

Finally, we examined the possible role of the second mechanism of DENV2 NS2B/NS3 protease inhibition, in which perturbing movement of the NS2B chain into the allosteric pocket area results

CPD# / pose	NS3-ASP 71	NS3-LYS 73	NS3-LYS 74	NS3-TRP 83	NS3-LEU 85	NS3-GLY 87	NS3-GLU 88	NS3-TRP 89	NS3-GLU 91	NS3-THR 118	NS3-THR 120	NS3-VAL 147	NS3-LEU 149	NS3-ASN 152	NS3-VAL 155	NS3-ALA 164	NS3-ILE 165	NS3-ASN 167
(1)/a				34	59	36							97					
(1)/b						100		98			33	98						93
(2)/a		98								46	47		97	73				167
(2)/b		44								84	73		96					
(3)/a														93				68
(3)/b			45											4				
(4)/a			48	57		34					70		31	119				
(4)/b													137	55		99	16	76
(5)													56	148				223
(6)/a			188			15		103				96	76	91		100		186
(6)/b	17	47					85	3					188	72		120		100
(7)/a		131									42			5				137
(7)/b		28	20											41		50		109
(8)			3					123					200	109		99		57
(9)			23	21				36					200	96		100		40
(10)		13	94				85						200	202		100		205
(11)			128	86									245	44		100		81
(12)			163	20									55	97				24

Grey colored bars show occupancies which are respectively to values:

<10% <30% <50% <75% <100% <125% <150% <199% >200%

Fig. 5. Hydrogen bonds occupancies[a] during the unrestrained 5 ns molecular dynamics simulations for the complexes of DENV2 NS2B/NS3 protease and the allosteric inhibitors. Depicted are data for the compounds (1)–(12) in relation to the allosteric site amino acids. ([a] When occupancy is lower than 100%, the hydrogen bond is sometimes broken in the course of the simulation; when the occupancy is higher than 100%, additional hydrogen bonds between the amino acid residue and the ligand molecule are created during simulation (for example, 200% for compound (8) – Leu149 means that before simulation there was one hydrogen bond, and second hydrogen bond had been created in course of simulation). To simplify picture, if there are more than one hydrogen bond between the ligand and the amino acid, their occupancies are merely summated).

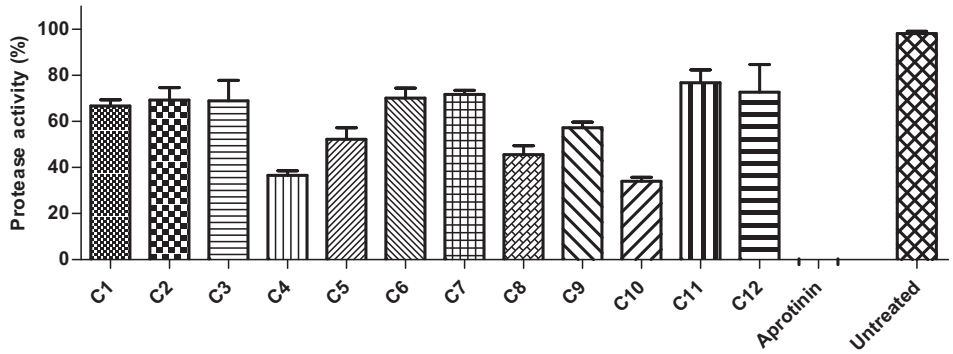

Fig. 6. Preliminary *in vitro* enzyme inhibition study using a common DENV2 NS2B/NS3 protease construct NS2B-GLY_4-SER-GLY_4-NS3pro. Results are represented as percentage of protease activity attained at 100 μM ligand concentrations.

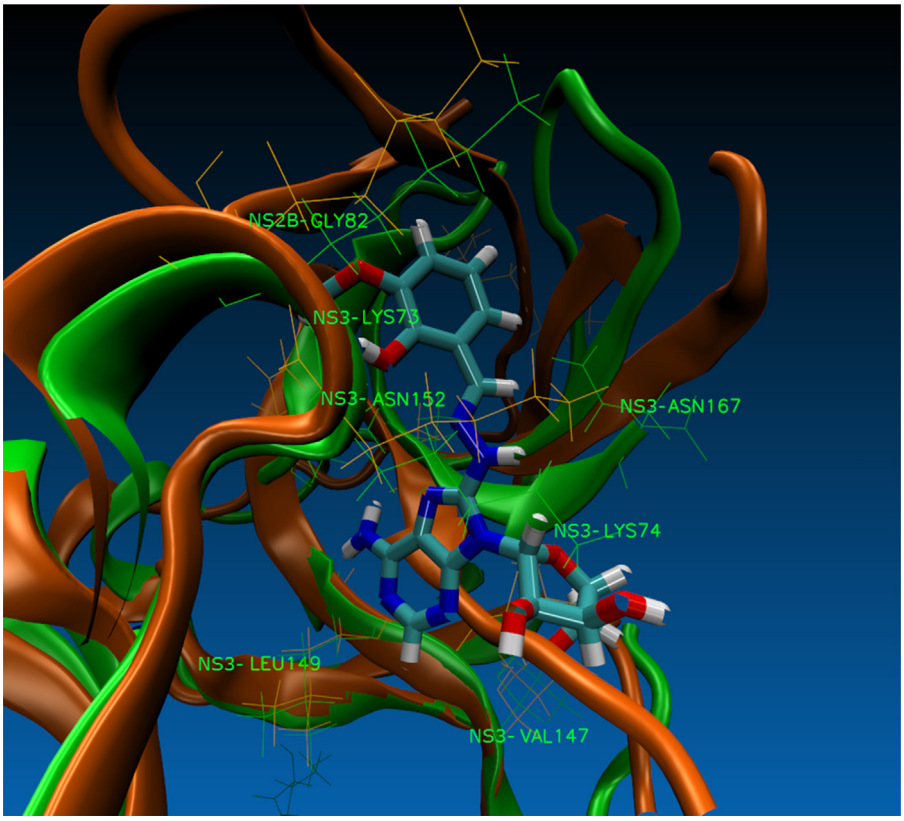

Fig. 7. Superposition of the "closed" (Wichapong et al.' homology model[a], orange ribbon), and "open" (green ribbon, 2FOM.PDB structure) conformations of DENV2 NS2B/NS3 protease in complex with inhibitor ZINC089185678 (Compound (10)). Interacting residues are highlighted. As it is indicated, binding of ZINC08918578 into the allosteric pocket may work also through additional mechanism of perturbing conformational motion of protein from the "open" to the "closed" conformation. ([a] The homology model of the "closed" conformation of DENV2 NS2B/NS3 protease was used for the comparison by permission of the authors of K. Wichapong, S. Pianwanit, W. Sippl, S. Kokpol. *Homology Modeling and Molecular Dynamics Simulations of Dengue Virus NS2B/NS3 Protease: Insight into Molecular Interaction*. **J. Mol. Rec.** 23(3), 283–300, 2010). (For interpretation of the references to color in this figure legend, the reader is referred to the web version of the article.)

in the "closed" conformation. For that purpose, structures of the protein–ligand complexes resulting from docking were superimposed on the structure of the "closed" conformation of the protease, modeled by Wichapong et al. [11]. The following molecular mechanisms may occur: (a) destabilizing contact between the C-terminal of NS2B and the allosteric pocket of the NS3pro domain; and (b) creating steric hindrance for the C-terminal of NS2B interacting with the allosteric pocket. Analysis of the superimposed structures (Fig. 7) showed, that for mechanism (a) the ligand should create hydrogen bonds with NS3-ASN152, already explored in our study and earlier [14]. For mechanism (b) the ligand should be situated between NS3-LEU149 and NS2B-GLY82, as exemplified by compound (10) in Fig. 7, and be at least 16 Å long. Since all of the identified allosteric inhibitors satisfy one or both of these rules, we propose that all of them might work through both general mechanisms.

4. Conclusion

In silico screening against the allosteric pocket of the DENV2 NS2B/NS3 protease led us to identify new ligands potentially able to bind it. Though SiteMap analysis of the protein surface indicated that the allosteric pocket has the highest drug affinity level (0.975), it is mainly hydrophilic, lined with many potentially interacting residues, and has a large buried volume, making drug discovery for this target a challenging task.

Our data with sugar-bound flavone and adenosilhydrazine derivatives indicates that such scaffolds might be particularly favorable for allosteric inhibition. It is interesting that ATP, identified as a top hit during sub-docking with a library of nucleosides, could bind to the allosteric pocket (data not shown). Glucose was identified as the top hit during sub-docking against a specifically generated library of 64 hexoses of varying stereo isomeric forms (data not shown).

We were able to study two feasible molecular mechanisms of inhibition. Each of the ligands we identified worked through both mechanisms: (a) creating hindrances for substrate interaction with the catalytic triad, or modulating the activity of the catalytic triad by electron density perturbation, and (b) interfering with the motion of the C-terminal of NS2B into the allosteric pocket during formation of the "closed" protein conformation.

Two parameters govern experimental allosteric inhibition activity: strength of binding (assessed as dG_{bind} by MM PB/GBSA calculations), and geometrical fitting into the underlying mechanism of inhibition (which is sequentially governed also by the general allosteric inhibition mechanisms). While these two parameters vary among the compounds found, the adenosine derivatives fit best with both parameters.

In summary, high throughput *in silico* screening and elucidation the mechanism of DENV2 NS2B/NS3 protease will contribute to the discovery of therapeutics against Dengue virus infection.

Acknowledgments

This work was supported by APEX funding (Malaysia Ministry of Higher Education) to the Centre for Chemical Biology, Universiti Sains Malaysia. M.A. and E.I.N. thank XESEDE for a generous grant of supercluster time (TG-MCB100110).

Appendix A. Supplementary data

Supplementary material related to this article can be found, in the online version, at http://dx.doi.org/10.1016/j.jmgm.2014.06.008.

References

[1] J.L. Deen, E. Harris, B. Wills, A. Balmaseda, S.N. Hammond, C. Rocha, N.M. Dung, N.T. Hung, T.T. Hien, J.J. Farrar, Lancet 368 (2006) 170.
[2] J.S. Mackenzie, D.J. Gubler, L.R. Petersen, Nat. Med. Suppl. 10 (2004) 98.
[3] K. Irie, P.M. Mohan, Y. Sasaguri, R. Putnak, R. Padmanabhan, Gene 75 (1989) 197.
[4] G. Katzenmeier, Dengue Bull. 28 (2004) 58.
[5] Z. Zuo, O.W. Liew, G. Chen, P.C. Chong, S.H. Lee, K. Chen, H. Jiang, C.M. Puah, W. Zhu, J. Virol. 83 (2009) 1060.
[6] R. Yusof, S. Clum, M. Wetzel, H.M. Murthy, R. Padmanabhan, J. Biol. Chem. 275 (2000) 9963.
[7] X.-C. Su, K. Ozawa, R. Qi, S.G. Vasudevan, S.P. Lim, G. Otting, PLoS Negl. Trop. Dis. 3 (12) (2009) 3.
[8] S. Chandramouli, J.S. Joseph, S. Daudenarde, J. Gatchalian, C. Cornillez-Ty, P. Kuhn, J. Virol. 84 (2010) 3059.
[9] O. Choksupmanee, K. Hodge, G. Katzenmeier, S. Chimnaronk, Biochemistry 51 (2012) 2840.
[10] C.G. Noble, C.C. Seh, A.T. Chao, P.Y. Shi, J. Virol. 86 (2012) 438.
[11] K. Wichapong, S. Pianwanit, W. Sippl, S. Kokpol, J. Mol. Recognit. 23 (2010) 283.
[12] D. Leung, K. Schroder, H. White, N.X. Fang, M.J. Stoermer, G. Abbenante, J.L. Martin, P.R. Young, D.P. Fairlie, J. Biol. Chem. 276 (2001) 45762.
[13] T.S. Kiat, R. Pippen, R. Yusof, H. Ibrahim, N. Khalid, N.A. Rahman, Bioorg. Med. Chem. Lett. 16 (2006) 3337.
[14] R. Othman, T.S. Kiat, N. Khalid, H.A. Wahab, R. Yusof, N.A. Rahman, J. Chem. Inf. Model. 48 (2008) 1582.
[15] P. Erbel, N. Schiering, A. D'Arcy, M. Renatus, M. Kroemer, S.P. Lim, Z. Yin, T.H. Keller, S.G. Vasudevan, U. Hommel, Nat. Struct. Mol. Biol. 13 (2006) 372.
[16] L.L.C. Schrödinger, Schrödinger Suite, 2011.
[17] J.J. Irwin, B.K. Shoichet, J. Chem. Inf. Model. 45 (2005) 177.
[18] W. Humphrey, A. Dalke, K. Schulten, J. Mol. Graphics 14 (1996) 33.
[19] T.J. Dolinsky, J.E. Nielsen, J.A. McCammon, N.A. Baker, Nucleic Acids Res. 32 (2004) W665.
[20] V. Zoete, M.A. Cuendet, A. Grosdidier, O. Michielin, J. Comput. Chem. 32 (2011) 2359.
[21] J.C. Phillips, R. Braun, W. Wang, J. Gumbart, E. Tajkhorshid, E. Villa, C. Chipot, R.D. Skeel, L. Kalé, K. Schulten, J. Comput. Chem. 26 (2005) 1781.
[22] D.A. Case, T.A. Darden, T.E. Cheatham III, C.L. Simmerling, J. Wang, R.E. Duke, R. Luo, R.C. Walker, W. Zhang, K.M. Merz, B. Roberts, B. Wang, S. Hayik, A. Roitberg, G. Seabra, I. Kolossvai, K.F. Wong, F. Paesani, J. Vanicek, J. Liu, X. Wu, S.R. Brozell, T. Steinbrecher, H. Gohlke, Q. Cai, X. Ye, J. Wang, M.-J. Hsieh, G. Cui, D.R. Roe, D.H. Mathews, M.G. Seetin, C. Sagui, V. Babin, T. Luchko, S. Gusarov, A. Kovalenko, P.A. Kollman, AMBER 11, 2010.
[23] Grace http://plasma-gate.weizmann.ac.il/Grace/. 2013.
[24] A. D'Arcy, M. Chaillet, N. Schiering, F. Villard, S.P. Lim, P. Lefeuvre, P. Erbel, Acta Crystallogr. F 62 (2006) 157.
[25] S.M. Tomlinson, R.D. Malmstrom, A. Russo, N. Mueller, Y.P. Pang, S.J. Watowich, Antivir. Res. 82 (2009) 110.